Characterization of the Interaction of Single Tryptophan Containing Mutants of IpaC from *Shigella flexneri* with Phospholipid Membranes†

Amanda Harrington,‡,§ Numukunda Darboe,‡,§ Roma Kenjale,‡ Wendy L. Picking,‡ C. Russell Middaugh,|| Susan Birket,‡ and William D. Picking*,‡

Departments of Molecular Biosciences and Pharmaceutical Chemistry, University of Kansas, Lawrence, Kansas 66045

Received June 30, 2005; Revised Manuscript Received November 14, 2005

ABSTRACT: *Shigella flexneri* causes dysentery after invading the epithelial cells of the human colon. Enterocyte invasion is induced by the bacterial effector IpaC (invasion plasmid antigen C), which triggers *Shigella* entry into epithelial cells by a rather poorly understood mechanism. IpaC is also involved in pathogen escape into the host cell cytoplasm following uptake, and this property may be reflected in its ability to disrupt phospholipid vesicles in vitro. Purified recombinant IpaC interacts with liposome vesicles to cause the release of small molecules trapped inside. This interaction requires that the liposomes possess an acidic phospholipid component. To better understand the events involved in the disruption of liposomes by IpaC, single tryptophan mutants were generated to permit the use of intrinsic fluorescence, circular dichroism, and ultraviolet absorption spectroscopies to examine the effect that phospholipid membrane association has on IpaC structure and stability. These mutants were also used to determine how amino acid substitutions within specific regions of IpaC influence its activity in vivo. The outcomes of this study include findings that cholesterol greatly impacts IpaC association with phospholipid membranes, tryptophan incorporation into specific regions of IpaC (especially near the C-terminus) can greatly impact its in vivo activity, and interaction with phospholipid membranes causes differing degrees of change in the fluorescence of tryptophan residues introduced at specific sites within IpaC. These data, together with fluorescence quenching analyses, provide new functional and structural information concerning IpaC and its insertion into phospholipid membranes.

Shigella flexneri is the causative agent of shigellosis, a mild to severe gastrointestinal syndrome of humans with worldwide public health importance (*1*, *2*). Following ingestion, *S. flexneri* travels to the human colon, where it crosses the colonic epithelial barrier via specialized microfold cells (*3*). Epithelial cell invasion then occurs as a result of localized actin polymerization at the site of bacterial contact with the cell (*4*, *5*). Actin polymerization is initiated when *S. flexneri* triggers activation of the host protein Cdc42, which induces the formation of filopodia that subsequently mature into lamellipodia by a Rac-dependent mechanism (*6*). These membrane ruffles coalesce to enclose the bacterium in a membrane-bound phagosome (*7*). *Shigella* subsequently lyses the phagosome to escape into the host cell cytoplasm (*8*). The bacterial invasion plasmid antigen proteins IpaB[1] and IpaC are implicated as effectors of *Shigella* entry (*9*−*11*) with IpaC possessing the majority of the biochemical properties that are consistent with its being the primary effector of *S. flexneri* entry (*6*, *12*−*16*).

Purified IpaC has been shown to enhance invasion of cultured cells by wild-type *S. flexneri* (*12*), promote global changes in the actin cytoskeleton of these cells (*15*), promote the uptake of noninvasive bacteria (*12*, *17*), and enhance the uptake of bacteria by cultured macrophages (*16*). In addition, IpaC can disrupt phospholipid vesicles (*13*, *18*), but it does so efficiently only when an acidic phospholipid component is present in the vesicles (*13*, *18*). A portion of IpaC that is required for interaction with and disruption of phospholipid membranes is its central hydrophobic region (*13*, *15*, *19*), which also appears to be important for overall protein folding and stability (*13*). Deletions of other portions of IpaC do not interfere with its ability to interact with or disrupt phospholipid membranes (A. T. Harrington, unpublished data), although they can have a major impact on IpaC's

† This work was supported by PHS Grants AI034428 and RR017708 (NIH COBRE Program in Protein Structure and Function).

* Corresponding author. Mailing address: Department of Molecular Biosciences, University of Kansas, 1200 Sunnyside Ave., Lawrence, KS 66045. Tel: (785) 864-3299. Fax: (785) 864-5294. E-mail: picking@ku.edu.

‡ Department of Molecular Biosciences.

§ A.H. and N.D. contributed equally to this work.

|| Department of Pharmaceutical Chemistry.

[1] Abbreviations: IpaB, invasion plasmid antigen B; IpaC, invasion plasmid antigen C; Trp, tryptophan; TSA, trypticase soy agar; TSB, trypticase soy broth; PCR, polymerase chain reaction; DOPC, 1,2-dioleoyl-*sn*-glycero-3-phosphocholine; DOPG, 1,2-dioleoyl-*sn*-glycero-3-[phospho-*rac*-(1-glycerol)]; CF, 6-carboxyfluorescein; MEM-glc, minimal essential medium supplemented with glucose; CD, circular dichroism; K_{SV}, Stern−Volmer steady-state quenching constant; F_0, starting fluorescence (prior to the addition of quenching agent); F, fluorescence at a given concentration of quenching agent; C_m, concentration of chemical denaturant giving the midpoint of transition between the folded state of a protein and its fully unfolded state; $\Delta G°$, Gibbs free energy for unfolding as a measure of intrinsic protein stability; T_m, temperature of the midpoint of transition between the folded state of a protein and its fully unfolded state.

10.1021/bi0512593 CCC: $33.50
Published on Web 12/15/2005

Table 1: PCR Primers Used in This Investigation

I40W	
primer 1	GAGAGACTCGAGCCAATGCGCTGCAATCTGCTG
primer 2	GAGAGACTCGAGCCACTTAATGTCGGTAAAAAT
A106W	
primer 1	GAGAGACTCGAGAGTCTTTCTTCTAATTGGGTTTCTTTAATTATTAGTGTAG
primer 2	GAGAGACTCGAGGGAAATATCCAGAGTGTTC
F136W	
primer 1	GAGAGACAATTGTCATTGATTGCGTGGGATGCTACAAAATCAGCTG
primer 2	GAGAGACAATTGAGAGCCCAATTTAGTTTCTG
L154W	
primer 1	GAGAGAAGGCCTGGCAGCCTGGTCATCAAGCATTACTGGAG
primer 2	GAGAGAAGGCCTTGCCGAACAATGGTCTCTG
S314W	
primer 1	GAGAGAGCTAGCCCAGGCCTGACTGATTAGTTG
primer 2	GAGAGAGCTAGCGCTGGCCTGACTGATTAG
K326W	
primer 1	GAGAGACTCGAGCCAAGATACTTGGGATGCTT
primer 2	GAGAGACTCGAGTCCCAAGCGACAAATCAAT
I336W	
primer 1	GAGAGACTCGAGCCATAATTGATTTGTCGCTTGGG
primer 2	GAGAGACTCGAGTTATTGAATATAATTGACAGCA
N341W	
primer 1	GAGAGACTCGAGTTATTGTGGATAATTGACAGCATCAACCA
primer 2	GAGAGACTCGAGTATTAATTGATTTGTCGCTTG
R362W	
primer 1	GAGAGAGGATCCTTAAGCCCAAATGTTACCAGCAATCTGAC
primer 2	GAGAGAGGATCCTCTAGAGTCGACCTGCAG

effector-related activities (*19*; W. L. Picking, unpublished data).

To better understand the biochemical basis for IpaC's ability to penetrate and disrupt phospholipid membranes, the influence of different lipid compositions on IpaC-mediated liposome disruption was investigated. It was found that cholesterol content clearly influences the rate and efficiency by which IpaC causes liposome disruption. To build upon these findings, single tryptophan (Trp) substitutions were introduced into IpaC, which possesses no Trp in its wild-type form. By generating single Trp mutants, it was anticipated that it would be possible to assess the roles that different regions of IpaC play in its interaction with phospholipid membranes. Single Trp incorporation has yielded valuable information on the structural features of other proteins (*20*) because it permits the use of fluorescence and other spectroscopic methods to directly monitor the microenvironment of specific regions within the protein in the presence and absence of phospholipid membranes. We have also assessed the effects of Trp incorporation at key sites on IpaC's structure, stability, and in vivo function.

EXPERIMENTAL PROCEDURES.

Materials. The *S. flexneri ipaC* mutant strain SF621 (*9*) was grown at 37 °C on trypticase soy agar (TSA) containing 0.025% Congo red. Henle 407 cells (ATCC CCL6) were propagated as monolayers in Eagle's modified minimal essential medium (MEM; Fisher Scientific, St. Louis, MO) supplemented with 10% calf serum (Life Technologies, Gaithersburg, MD) and grown in a 5% CO_2 environment. PCR SuperMix High Fidelity and oligonucleotides were purchased from Invitrogen (Carlsbad, CA) and Clonables 2x Ligation Premix and NovaBlue competent *Escherichia coli* from Novagen (Madison, WI). 1,2-Dioleoyl-*sn*-glycero-3-phosphocholine (DOPC), 1,2-dioleoyl-*sn*-glycero-3-[phospho-*rac*-(1-glycerol)] (DOPG), and brominated phosphatidylcholine lipids (6,7 and 9,10 diBr-PC) were obtained from Avanti Polar-Lipids, Inc. (Alabaster, AL). Cholesterol and sodium iodide were from Sigma Chemical Company (St. Louis, MO). 6-Carboxyfluorescein (CF) was from Molecular Probes (Eugene, OR). All other chemicals were reagent grade.

Generation of IpaC Single Trp Mutants. All *ipaC* Trp substitution mutants were generated using inverse PCR with pWPsfc′ (*21*) as the template and primers encoding GAGAGA and a restriction site flanking the codon to be mutated. The primers used for this study are listed in Table 1. A linear plasmid was thus amplified by PCR, restriction digested, intramolecularly ligated, and transformed into *E. coli* NovaBlue. The GAGAGA sequence present at the ends of the resulting PCR products allowed improved efficiency in restriction digestion, and subsequent closure of the linear plasmid prepared by this method. The resulting plasmid was electroporated into *S. flexneri* SF621. Ampicillin was used to select for the recombinant plasmid and kanamycin to select for the *S. flexneri* virulence plasmid with *ipaC* deleted (*9*). The restriction enzymes used here were mutant-specific so as to introduce the minimal amount of change in the IpaC primary sequence. Trp mutants at positions 40 and 106 were generated by introducing the restriction site *Xho*I (encoding Leu and Glu) in addition to the substitution of the Trp. Trp substitutions at positions 136 and 154 were created using the naturally occurring restriction sites *Stu*I and *Mfe*I, respectively. Mutants at positions 314, 326, and 341 were generated by introducing an *Nhe*I site to create a silent mutation (*13*) proximate to the Trp substitution. The I336W mutant was generated using the same method, except that *Xho*I was used as the restriction site. The R362W mutation was introduced directly via the DNA primer used for amplification.

The rationale for introducing Trp residues at these specific positions was as follows: (1) position 40 is near the N-terminus of IpaC in a region that is dispensable for IpaC function in vivo (*21*) and is largely unfolded based on

preliminary 1-D NMR spectroscopy (data not shown); (2) position 106 lies at the start of the central hydrophobic region and predicted transmembrane helix; (3) position 136 is in the same hydrophobic region but lies between the predicted transmembrane helices; position 154 is at the end of the hydrophobic region and lies near the end of a second transmembrane helix (*19*); (4) position 314 lies just upstream of a predicted coiled-coil region near the IpaC C-terminus; positions 326 and 336 lie within this predicted coiled-coil; position 341 is positioned at the very end of the predicted coiled-coil (*13*) and at the start of a region believed to be involved in triggering cytoskeletal changes in epithelial cells (data not shown); and position 362 is the penultimate amino acid of IpaC and may be involved in effector function (data not shown). Other regions, including the central, largely hydrophilic region of IpaC between amino acids 170 and 290 were not targeted for Trp incorporation since they can be deleted without eliminating IpaC function (*19*).

Preparation of Affinity-Purified Recombinant Proteins. The plasmid used to prepare recombinant IpaC has been described (*12*, *14*, *19*). The *ipaC* genes with the single Trp mutations were subcloned from pWPsf into pET15b, which encodes a 20 amino acid leader sequence possessing six tandem His residues. All new plasmids were transformed into *E. coli* BL21(DE3) for protein production. Recombinant proteins were purified using the N-terminal His_6 tag by nickel-chelation chromatography as described in detail previously (*21*). Purified proteins were step-dialyzed against 10 mM phosphate, pH 7.2, 150 mM NaCl (PBS) to remove the 6 M urea (4 M, 2 M, 1 M, 0.5 M, and then to 0 M urea). In some cases, the urea concentration was reduced to 2 M and experiments were carried out by rapid dilution into buffer (in the presence or absence of liposomes). For secondary structure analysis, the urea was completely removed but solubility was maintained by adding 0.1% Tween-20. The inclusion of Tween-20 did not alter the secondary content of IpaC as detected by CD and did not affect its unfolding temperature.

Preparation of Phospholipid Vesicles. Phospholipid vesicles were generated by extrusion essentially as described (*13*). DOPC and DOPG in chloroform were dried under nitrogen and then vacuum for 3 h to create lipid films. Lipid films were also created containing 1%−15% cholesterol. For cholesterol containing films, the percentage of DOPG was held constant at 25%, while the concentration of DOPC was adjusted according to the cholesterol content. Films were hydrated in PBS and dispersed in a bath sonicator for 30 min or dismembranating sonicator for 10 s prior to extrusion through a 100 nm pore membrane at least 10 times at 45 °C. Liposomes were diluted 1:3 in PBS. During preparation of liposomes containing fluorescein, the lipid films were hydrated in a solution containing 100 mM 6-carboxyfluorescein (CF) which had been solublized at pH 7.2 in PBS. After extrusion, the excess dye was separated from the bulk liposomes by gel filtration using Sephadex G-50 equilibrated with PBS. The liposomes used for investigating IpaC insertion were composed of 50% DOPC and 50% DOPG since these phospholipids permitted maximal insertion of IpaC as judged by the release of CF following protein addition. In a few cases, as indicated, liposomes with a smaller amount of DOPG were used.

Monitoring the Release of CF from Phospholipid Vesicles. Release of CF from phospholipid vesicles (*13*) was monitored using a SPEX FluoroMax fluorometer (JY/Spex, Edison, NJ). At high concentrations within liposomes, encapsulated fluorescein is self-quenched, which is relieved by disruption of the liposomes due to rapid dilution of the CF. Liposomes (approximately 100 μM) were suspended in PBS, and initial baseline fluorescence was observed for 30 s to 1 min to confirm liposome integrity. Purified IpaC mutants or 0.1% Triton X-100 (as a positive control for liposome disruption) was added after 1 min, and the release of CF was monitored as a time-dependent increase in fluorescence. CF fluorescence was monitored using 492 nm as the excitation wavelength and 517 nm as the wavelength for emission detection.

Bacterial Invasion of Cultured Cells. The level of *S. flexneri* invasion of cultured cells was monitored as described (*21*). *S. flexneri ipaC* mutants harboring plasmids expressing *ipaC* or one of its mutants were grown in trypticase soy broth (TSB) with 100 μg/mL Amp and 50 μg/mL Kan to an A_{600} of 0.5. The bacteria were diluted into serum-free MEM containing 0.45% glucose (MEM-glc) and centrifuged onto preconfluent Henle 407 cell monolayers (multiplicity of infection $\sim$ 10), and incubated with the cells for 30 min at 37 °C. Free bacteria were removed by aspiration and the monolayers washed with MEM containing 5% calf serum and 50 μg/mL gentamycin. The cells were incubated in the final gentamycin (50 μg/mL) wash for 1 h to kill adherent but noninternalized bacteria and then rinsed with MEM-glc. The cells were then overlaid with 250 μL of 0.5% agarose in water and then with 0.5% agar containing LB medium. After overnight incubation at 37 °C, the internalized bacteria that formed subsurface colonies were counted.

Measurement of Contact-Mediated Hemolysis. Hemolysis was measured according to Sansonetti (*8*). Bacteria were grown overnight on TSA-Congo red plates, and a single red colony was used to inoculate TSB. Mid-log phase bacteria were collected by centrifugation and suspended in PBS at 2.5% of the original volume. Sheep erythrocytes were washed and resuspended in PBS at 1×10^{10} cells/mL. Erythrocytes and bacteria (50 μL each) were added to microtiter wells and the plates centrifuged at 2200*g* for 15 min at 20 °C, and the plates were incubated at 37 °C for 2 h. The cells were then suspended by addition of 90 μL of cold PBS, and the plates were centrifuged again at 2200*g* at 15 °C for 15 min. The supernatant fraction (100 μL) was transferred to a second microtiter plate and absorbance of the released hemoglobin measured at 545 nm.

Circular Dichroism Spectroscopy. Far UV CD spectra and thermal unfolding monitored at 222 nm were performed using a Jasco J720 spectropolarimeter (Jasco Inc., Easton, MD). Far UV CD spectra were recorded from 260 to 190 nm at a scan rate of 15−20 nm/min using a 0.01 cm path length cell. Spectra were acquired in triplicate and averaged. The thermally induced unfolding curves were acquired using a 0.1 cm path length cell with a temperature ramping rate of 15 °C/h. The protein concentration in all cases was between 2 and 10 μM. CD signals were converted to molar ellipticities, and the unfolding transitions were analyzed using Jasco Spectral Manager software. The CONTIN (*22*), SELCON (*23*), and CDSSTR (*24*) programs were used to estimate secondary structure content for IpaC as previously described (*13*).

In urea-induced unfolding experiments, the urea concentration was determined based on the refractive index of the solution using a Bausch & Lomb refractometer and calculated using the method of Pace (*25*). Spectra of protein solutions with various urea concentrations were acquired as described above, and the CD signal at 222 nm was plotted against urea concentration. To determine the free energy of unfolding (ΔG) in the absence of denaturant, data were nonlinearly fitted to a two-state unfolding model (using Igor Pro software) (*25*).

Fluorescence Spectroscopy. Fluorescence emission spectra were acquired using a PTI QM-1 spectrofluorometer (Lawrenceville, NJ) equipped with Felix software. Samples were excited at 295 nm (> 95% Trp emission) and the emission spectra collected between 305 and 400 nm at a scan rate of 30 nm/min using a 1 cm path length cell. In thermal studies, spectra were obtained at 2.5 °C intervals beginning at 10 °C. Each spectrum is an average of two scans. Buffer spectra at given temperatures were subtracted from the sample spectra at the same temperatures using the Felix software. Depending upon protein concentration, slit widths were set between 4 and 6 nm. Alternatively, fluorescence spectra were obtained using a Spex FluoroMax spectrophotometer for determination of emission maxima with and without liposomes.

Fluorescence Quenching Analyses. To monitor the ability of small solutes to interact with Trp residues incorporated into IpaC, steady-state fluorescence quenching was used (*26*). Briefly, the fluorescence emission of a sample was determined in the absence or presence of increasing concentrations of sodium iodide, which is a useful fluorescence quenching agent (*27*). The degree of quenching in this case was determined by plotting F_0/F versus the concentration of sodium iodide, where F_0 is the starting (unquenched) fluorescence intensity of the single Trp containing IpaC mutant and F is the fluorescence intensity at a given concentration of quenching agent ([Q]). The Stern−Volmer quenching constant (K_{SV}) was determined from the slope of the resulting plot according to the relationship $F_0/F = 1 + K_{SV}[Q]$. K_{SV} thus provides a measure of solvent accessibility to the Trp residues of IpaC (*28*). Alternatively, the interaction of single Trp mutants of IpaC was examined for the fluorescence emission of the mutants when incorporated into liposomes containing dibrominated (diBr) phosphatidylcholine lipids possessing bromine moieties at either positions 6 and 7 (6,7 diBr-PC) or positions 9 and 10 (9,10 diBr-PC) (*27*). The relative fluorescence, or quenching of fluorescence for liposomes containing (25%) of either of these lipids provided an initial basis for estimating the depth of penetration of IpaC (i.e. specific Trp residues within IpaC) into artificial phospholipid vesicles. Some problems were encountered with making precise measurements here (especially with 11,12 diBr-PC) in that incorporation of these modified lipids appeared to compromise the integrity of the resulting liposomes. Nevertheless, the data are presented as percent quenching of total fluorescence by diBr-PC according to $(1 - F/F_0) \times 100$, where F is the emission intensity of Trp in the presence of liposomes containing diBr-PC and F_0 is the emission intensity of Trp in the presence of liposomes lacking the brominated lipid quenching agent.

UV Absorption Second Derivative Analysis. Protein concentration determination and second derivative UV spectroscopy were carried out using an Agilent 8453 UV−visible spectrophotometer (Palo Alto, CA) (*13*). Protein concentrations were calculated using extinction coefficients of 5960 M^{-1} cm^{-1} and 11460 M^{-1} cm^{-1} at 280 nm for IpaC and the tryptophan mutants, respectively. This is based on the molar extinction coefficient being equal to the number of Trp residues multiplied by 5500, the number of tyrosines multiplied by 1490, and the number of cysteines multiplied by 125. IpaC has four native Tyr residues. In temperature perturbation studies, spectra were acquired over a temperature range of 10 to 90 °C at 2.5 °C (±0.1 °C at each temperature examined) intervals within a 1 cm path length cell with continuous stirring. Each spectrum was collected with an integration time of 25 s after a 5 min equilibration time. Using Chemstation software (Agilent), spectra were converted to second derivatives using a nine-point data filter and a fifth degree Savitzky−Golay polynomial, and subsequently fitted to a cubic function with a 99-point data interpolation. The resolution of the final spectra was ±0.01 nm. Data were imported into Microcal Origin, where peak positions were measured (*29*).

UV absorption second derivative analysis is particularly attractive for the given investigation because it can be used in mildly aggregating systems since it is not very sensitive to spectral artifacts such as light scattering, which occur as a result of protein aggregation (*29*, *30*). These spectra display two phenylalanine minima, two tyrosine minima, one Tyr/Trp minimum, and one tryptophan minimum. In this investigation, analysis of the single Trp minimum was emphasized to focus on the Trp containing sites.

Potentially Hazardous Procedures. The primary hazard encountered in these studies is the use of the bacterial pathogen *S. flexneri*, which requires handling under biosafety level 2 conditions. Because of the relatively low dose of *S. flexneri* required for human infection, even mutant strains of the organisms were handled using BSL-2 protocols as outlined by the Centers for Disease Control and Prevention (*31*). *S. flexneri* is not a designated "select agent" and thus does not require special permits for its use under accepted laboratory conditions.

RESULTS

Generation of Single Tryptophan Mutants of IpaC. To better characterize its interaction with phospholipid membranes using fluorescence spectroscopy, tryptophan (Trp) residues were introduced at specific sites into the *Shigella* invasion protein IpaC. Since native IpaC lacks Trp, changes in the emission properties of the Trp residues introduced at defined sites can be used to probe the role of individual parts of IpaC in membrane interactions. Trp fluorescence is directly influenced by the polarity of its immediate surroundings, making it a sensitive intrinsic probe of its microenvironment (*32*). Regions chosen for the introduction of Trp included (a) a site near the IpaC N-terminal region that is associated with secretion, chaperone binding, and IpaB binding (*21*); (b) three distinct positions within the central nonpolar region known to be important for membrane interactions (*19*) and protein stability (*13*); (c) one position located upstream from a predicted coiled-coil trimerization domain (*33*); (d) three regions located within the predicted coiled-coil trimerization domain that may be important for

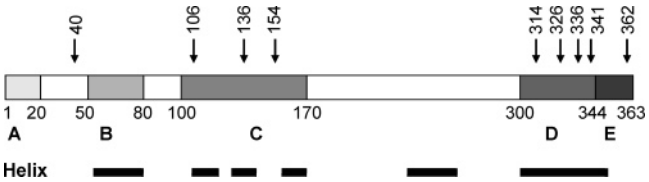

FIGURE 1: A schematic model of the functional organization of IpaC. Functionally important regions of IpaC include (A) an N-terminal TTSS export signal; (B) a region involved in chaperone binding; (C) a central hydrophobic region involved in overall stabilization and membrane association; (D) a region containing a predicted coiled-coil that allows IpaC oligomerization; and (E) a C-terminal tail that is important for signaling entry into target cells. Trp was used to replace existing residues at the positions indicated by the arrows. Based on in silico secondary structure analysis, the regions indicated by the lower black bars are predicted to form α-helices; however, a peptide composed of residues 1 to 100 is known to lack any significant helical structure based on one-dimensional NMR analysis (unpublished result). It should be noted, however, that IpaC association with binding partners may have a major impact on its overall secondary structure content. Only sporadic beta structure was predicted to occur within IpaC (not shown).

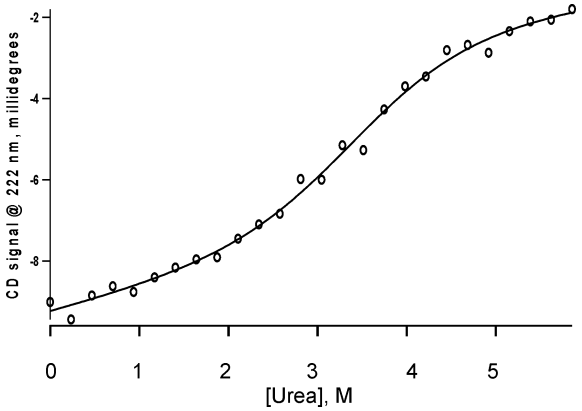

FIGURE 2: Conformational perturbation of IpaC occurs as a function of increasing the urea concentration. IpaC secondary structure was monitored by CD spectroscopy using a 0.1 cm path length cell in PBS buffer, pH 7.2. The free energy of unfolding was calculated to be 4 ± 1 kcal/mol. The open circles are experimental data points, and the solid line is the fit to the data using a two-state model.

IpaC oligomerization (*13*, *33*); and (e) the penultimate C-terminal residue of IpaC which may be important for its effector function (K. Flentie and W. L. Picking, unpublished data). The precise placement of these Trp residues and a functional map of IpaC are provided in Figure 1, and the rationale for this placement is provided in the Experimental Procedures section.

One difficulty in working with IpaC is its low solubility. For the experiments described in this study, IpaC was prepared from inclusion bodies following solubilization with urea. To maintain IpaC at high concentrations, much of the urea could be removed, but below a concentration of 2 M the protein begins to aggregate and precipitate from solution. Subsequent experiments requiring purified IpaC were then carried out following rapid dilution of the IpaC sample to a protein concentration of approximately 1 μM into a buffered solution having a final urea concentration less than 0.2 M. At these relatively low protein concentrations, IpaC aggregation was rarely detected.

Interestingly, urea-induced unfolding studies (Figure 2) showed that IpaC has an intrinsic stability ($\Delta G°$) of about 4 ± 1 kcal/mol with a midpoint of denaturation (C_m) at about 3.3 M urea. This $\Delta G°$ value, although on the lower end of values usually encountered, is comparable to those of other small globular proteins despite the low solubility of IpaC (*34*). At 0.2 M urea, IpaC structure is similar to that of the native state (absence of urea) as shown in Figure 2. Fluorescence quenching experiments also indicated that the solvent accessibility of the Trp residues within the hydrophobic region of IpaC, at positions 106, 136, and 154, is unaffected by the presence of low concentrations of urea, even up to 1 or 2 M (data not shown). These results suggest that the inclusion of low concentrations of urea in experiments examining IpaC's ability to interact with phospholipid membranes does not compromise the relevance of the results with respect to IpaC folding.

Table 2: Functional Analysis of the IpaC Single Trp Mutants Produced in *S. flexneri* SF621

Trp mutant	relative invasion[a]	contact hemolysis[b]
IpaC	100 ± 10[c]	100 ± 5
I40W	97 ± 5	82 ± 18
A106W	90 ± 12	88 ± 19
F136W	85 ± 18	70 ± 27
L154W	63 ± 7*	88 ± 10
S314W	68 ± 9*	57 ± 2***
K326W	68 ± 17*	42 ± 14***
I336W	90 ± 14	91 ± 16
N341W	3 ± 3**	60 ± 28***
R362W	7 ± 2**	82 ± 25

[a] Invasion was determined using a standard gentamycin protection assay (*21*) with all data normalized to the rate of invasion for *S. flexneri* SF621 (*ipaC* mutant) harboring pWPsfC. [b] Contact hemolysis was determined according to Sansonetti (*8*). The data are presented as relative hemolysis compared to SF621 expressing native *ipaC* (*21*). [c] Statistics: unpaired Student's *t* test, *invasion *P* value ≤ 0.05, ** invasion *P* value ≤ 0.0001, ***contact hemolysis *P* value ≤ 0.05. $n = 3$ in all cases.

Incorporation of Trp into Some Sites Influences IpaC's Function. The effect of Trp substitutions on the in vivo function of IpaC was assessed by expressing each gene in the *S. flexneri ipaC* null mutant strain SF621 (*9*). The IpaC virulence related activities tested were restoration of invasion of cultured cells and contact-hemolytic activity using sheep erythrocytes. Seven out of nine of the mutants retained a significant level of invasiveness for SF621 (Table 2). All of the purified proteins displayed CD spectra identical to that of wild-type recombinant IpaC (data not shown), suggesting that the observed negative effects of the mutations on IpaC's in vivo activity are not due to a gross disruption of IpaC structure. Despite normal folding, placement of Trp at positions 341 and 362 (in IpaC's putative coiled-coil and effector regions, respectively) resulted in nearly complete elimination of invasion activity (Table 2). The elimination of invasion for Trp mutants 341 and 362 suggests that IpaC's immediate C-terminus is critical for *Shigella* uptake by mammalian cells. In addition, the Trp replacements at residues 154, 314, and 326 significantly reduced IpaC-mediated invasiveness (Table 2). All the mutants described here retained a substantial portion of SF621's ability to lyse erythrocytes regardless of whether they restored invasiveness (Table 2). Hemolysis efficiency was, however, moderately reduced for some mutants, the most notable reduction (defined in this case as greater than 50% and with a *P* value of ≤0.03 using Student's *t* test) being the substitution at

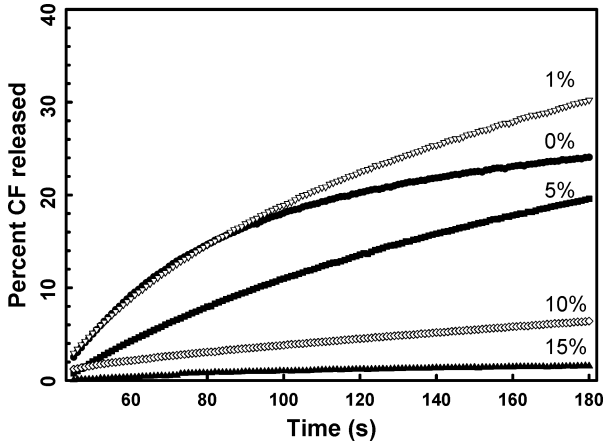

FIGURE 3: IpaC-dependent release of CF from liposomes is reduced when the amount of cholesterol is raised. Purified recombinant IpaC (1 μM) was incubated with CF-containing liposomes composed of DOPC (variable), 25% DOPG, and increasing amounts of cholesterol: 0%, filled circles; 1%, open triangles; 5%, filled squares; 10%, diamonds; and 15%, filled triangles. The release of CF was then monitored as a time-dependent increase in fluorescence emission. The data shown are from a single experiment, but are representative of data obtained in three independent analyses.

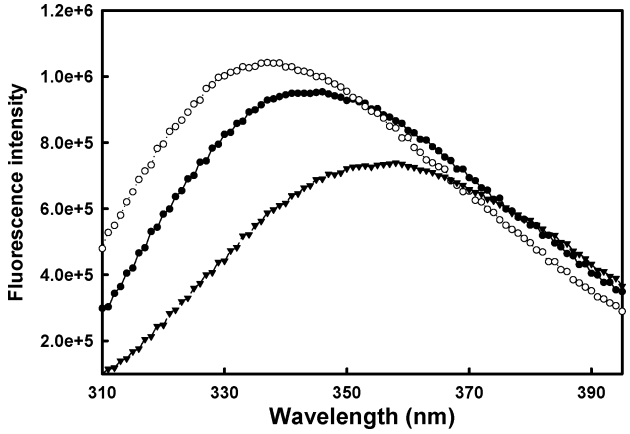

FIGURE 4: Representative fluorescence spectra of the IpaC mutant I336W (1 μM protein). A spectral scan of the recombinant protein in aqueous solution alone exhibits maximum Trp fluorescence around 345 nm (filled circles). Liposome addition causes the Trp fluorescence emission maximum to shift to around 338 nm (open circles). In contrast, when the protein is present in 6 M urea, the Trp fluorescence emission displays a red shift to around 356 nm (filled triangles).

position 326 (K326W), which is located within IpaC's predicted coiled-coil.

All of the Purified IpaC Trp Mutants Disrupt Phospholipid Vesicles, and the Inclusion of Cholesterol Influences IpaC's Ability To Disrupt Liposomes. The ability of IpaC to disrupt the integrity of phospholipid bilayers can be determined by monitoring the release of 6-carboxyfluorescein (CF) trapped within liposomes where it undergoes concentration-dependent auto-quenching (*13*, *18*). Release of CF from the liposomes causes its rapid dilution, giving rise to increased fluorescence. Almost complete release of CF can be achieved by the addition of IpaC when the liposomes contain 50% acidic phospholipids (*13*). In contrast, IpaC poorly disrupts liposomes composed of only neutral phospholipids (*13*, *18*), although it does associate with Langmuir monolayers composed only of DOPC (*15*). In the initial experiments used in this study, the liposomes were composed of 70% DOPC, 25% DOPG, and 5% cholesterol. It turned out, however, that while the addition of cholesterol greatly enhanced the stability of the liposomes (as indicated by an increase in usable lifetime), it appears to decrease the efficiency by which IpaC caused liposome disruption. Thus, subsequent analysis of the fluorescence of IpaC Trp mutants in the presence of liposomes was done using 50:50 DOPC/DOPG liposomes lacking cholesterol, unless otherwise stated.

As previously reported, increasing the acidic phospholipid content to 50% (in the absence of cholesterol) allowed IpaC to cause complete release of CF, as determined by comparison with detergent-treated liposomes (*13*). Elimination of the acidic phospholipid component largely prevented IpaC-mediated liposome disruption (*13*). It was found, however, that IpaC's interaction with liposomes is influenced not only by the surface charge of the CF-containing liposomes but also by the presence of cholesterol. To assess the influence that cholesterol has on the interaction between IpaC and liposomes, the cholesterol content was varied and the ability of wild-type IpaC to cause CF release was again monitored. As shown in Figure 3, the highest initial rates of CF release caused by IpaC occur when cholesterol levels are relatively low in the liposomes (0−1%), but the largest total release of CF is seen with 1% cholesterol (88% total release) followed by 5% cholesterol (68%) and then no cholesterol (26%) in liposomes having a 25% DOPG content. Beyond 5% cholesterol, IpaC's ability to cause liposome disruption rapidly diminishes (Figure 3). Although 1% and 5% cholesterol increase the total release of CF caused by IpaC, the amount of time needed to achieve maximal release greatly increases in the presence of cholesterol (approximately 6 min with 1% cholesterol, 7 min with 5% cholesterol, and 2.5 min with no cholesterol). These are interesting findings since it has been suggested that the initial steps of *Shigella* infection may occur at cholesterol-rich lipid rafts (*35*, *36*). IpaC's partner invasin IpaB appears to interact with liposomes in the presence or absence of cholesterol, but with cholesterol possibly enhancing the disruption event (A. T. Harrington, unpublished data). IpaB and its homologue from *Salmonella*, SipB, are also reported to be cholesterol-binding proteins (*37*), which is consistent with the activity of the pore-forming toxins that they have been compared to. Nevertheless, IpaC is also able to interact with cholesterol-containing membranes.

Assessing the Environment of the Different IpaC Single Tryptophan Mutants by Fluorescence Spectroscopy. To demonstrate the influence of microenvironment on the fluorescent moiety of each IpaC Trp mutant, emission spectra were monitored in aqueous solution, following the addition of liposomes, and in the presence of 6 M urea to induce protein unfolding. Incubation with liposomes was for at least 10 min, which ensured maximum IpaC interaction. Representative data for one Trp mutant (I336W) is shown in Figure 4. For this mutant, the addition of liposomes causes a 7.6-nm blue shift in Trp emission. The addition of urea caused a major (10.1-nm) red shift in the emission maximum, which is consistent with a solvent-exposed indole side chain. These data indicate that the Trp residue of I336W is already located within a relatively nonpolar environment, while membrane insertion caused a significant increase in local hydrophobicity and urea induced nearly complete exposure of the Trp residue to the aqueous environment.

Table 3: Fluorescence Emission Wavelengths for the Different IpaC Single Trp Mutants in the Absence and Presence of Liposomes and Urea

mutant	wavelength[a,b]	liposomes added[a,b]	change (nm)	urea added to 6 M[a,c]
I40W	344.3 ± 0.4	342.7 ± 0.8	−1.6	355.4
A106W	342.5 ± 0.5	338.8 ± 0.9	−3.7	359.5
F136W	342.9 ± 0.4	338.3 ± 0.5	−4.6	358.5
L154W	342.2 ± 0.7	341.5 ± 0.4	−0.7	358.3
S314W	345.1 ± 0.4	340.6 ± 1.2	−4.5	359.3
K326W	344.8 ± 0.4	338.4 ± 0.7	−6.4	358.7
I336W	345.7 ± 0.3	338.1 ± 0.8	−7.6	355.8
N341W	344.3 ± 0.3	338.2 ± 1.1	−6.1	355.5
R362W	344.2 ± 0.5	337.7 + 0.9	−6.5	356.2

[a] The fluorescence emission maximum is presented as wavelength maximum in nm. Wild-type IpaC possesses no Trp residues and therefore does not possess a related peak. [b] $n \geq 3$. [c] $n = 2$.

From the overall data summarized in Table 3, amino acid positions 106, 136, and 154, each located within IpaC's predicted central hydrophobic region, are present within a slightly more nonpolar environment than the other Trp residues as indicated by their slightly blue-shifted emission spectra relative to the Trp residues located at other positions. All of the Trp residues introduced into IpaC had emission maxima between 342 and 346 nm in the absence of liposomes or urea (Table 3). To evaluate potential changes in the Trp environments following IpaC interaction with membranes, all mutants were incubated with liposomes so that their emission maxima could be compared with those of the IpaC mutants in the absence of liposomes (Table 3). Each was also examined in the presence of urea to determine the effect of exposure to the solvent on Trp emission.

All of the Trp mutants displayed blue shifts in their emission maxima upon liposome addition, suggesting entry into a less polar environment. Some mutants, however, displayed much greater shifts, which could indicate entry into the lipid bilayer interior. The smallest blue shifts were seen for I40W and L154W (Table 3), perhaps suggesting that the IpaC N-terminus and end of the IpaC hydrophobic region do not enter the membrane interior. In contrast, the C-terminal Trp replacements displayed larger blue shifts, perhaps indicating entry into the phospholipid bilayer. On the other hand, all the Trp mutants displayed major red shifts in their emission spectra upon the addition of urea (Table 3).

Fluorescence Quenching Analysis. To better understand the relationship between Trp spectral shifts and possible insertion of IpaC into liposomes, fluorescence quenching induced by potassium iodide was performed (Table 4). The Trp residue at position 40 was clearly the most accessible in the absence of liposomes, having a Stern−Volmer quenching constant of 6.18 M^{-1} (Table 4). Consistent with the very small blue shift upon the addition of 50:50 DOPC/DOPG liposomes, I40W remained accessible to iodide quenching following liposome addition (Table 4), indicating that it does not enter the membrane interior. The Trp residues having the greatest increase in protection from iodide quenching following the addition of liposomes, starting with the most protected, were at positions 106, 326, 336, and 314 (see Table 4). These data are consistent with the spectral shifts reported in Table 3. The remaining Trp residues were partially protected by iodide quenching following liposome addition, which suggests either moderate interaction with the liposomes or the induction of conformational changes in IpaC following liposome association. The latter is a possibility for the IpaC mutants N341W and R362W, which display significant blue shifts, but are only modestly protected from quenching by iodide upon liposome addition (Table 4).

Table 4: Iodide Fluorescence Quenching Analysis

IpaC mutant	K_{SV} (M^{-1})[a]	
	alone	liposomes added
I40W	6.18 ± 0.5	5.70 ± 1.5
A106W	3.37 ± 0.3	1.36 ± 0.4
F136W	4.15 ± 0.2	3.29 ± 0.3
L154W	4.38 ± 0.3	3.05 ± 0.3
S314W	4.19 ± 0.2	2.37 ± 0.2
K326W	4.30 ± 0.3	1.78 ± 0.3
I336W	2.65 ± 0.2	1.49 ± 0.2
N341W	3.92 ± 0.2	2.73 ± 0.2
R362W	3.61 ± 0.2	2.63 ± 0.3

[a] The K_{SV} values shown are an average ± SD of two experiments.

Table 5: Relative Fluorescence upon Insertion into Liposomes Containing Brominated DOPC

IpaC mutant	% quenching[a,b] lipid incorporated into liposomes	
	6,7	9,10
I40W	0	0
A106W	5	34
F136W	0	0
L154W	−1	0
S314W	4	0
K326W	0	0
I336W	14	10
N341W	20	10
R362W	3	5

[a] Percent quenching was calculated as $(1 - F/F_0) \times 100 =$ % of total fluorescence quenched. [b] All values are ±20% of the value shown, $n = 2$.

To complement the iodide quenching experiments described above, quenching by membrane integrated dibrominated lipids was performed in an attempt to determine the depth at which the different Trp residues might enter the liposome membranes (see Table 5). When IpaC was incorporated into liposomes containing no quenching agent and then liposomes containing 25% diBr-PC, the only residue that displayed significant quenching of total fluorescence by (9,10diBr)PC was A106W, which is consistent with the possibility that this residue enters rather deeply into the hydrophobic core of the liposome. Trp residues near the IpaC C-terminus, especially I336W and N342W, appeared to be modestly quenched by (6,7diBr)PC-containing liposomes, which is consistent with the possibility that they interact at the liposome surface and do not penetrate deeply into the bilayer core. Unfortunately, the apparent negative impact that the (11,12diBr)PC lipids had on liposome integrity made additional experiments difficult to interpret. For liposomes possessing (11,12diBr)PC, large errors were seen for the quenching of all of the Trp mutants (not shown), and when CF release was monitored for these liposomes in the absence of protein, baseline values appeared to fluctuate considerably. The reason for these observations is unclear since this does not seem to have been previously reported.

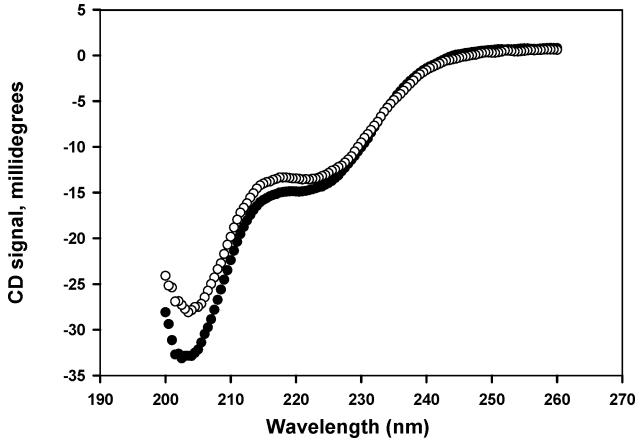

FIGURE 5: Far-UV circular dichroism spectra of IpaC (19 μM) alone in PBS at pH 7.2 (closed circles) and IpaC in the presence of liposomes (50:50 DOPC/DOPG) (open circles). The CD spectra were acquired at 10 °C with a scan rate of 20 nm/min using a 0.1 cm path length cell. The spectra shown are an average of two spectra taken under identical conditions.

CD Spectroscopy. The CD spectrum of IpaC at 10 °C shows minima at 222 and 203 nm, suggesting the presence of an α-helix component (Figure 5). The relatively high 203 to 222 nm signal ratio also suggests the presence of a significant amount of random structure. Previously, it was reported that IpaC possesses approximately 10% α-helix, 34% β-sheet, 22% turn, and 32% random structure at 20 °C in the absence of detergent (*13*). To determine whether Trp introduction alters IpaC stability, thermal melts using CD were performed. Unfortunately, protein aggregation with IpaC can compromise the resulting data. Therefore, Tween-20 was added as an inhibitor of aggregation. Addition of this mild detergent did not greatly influence overall secondary structure content (data not shown), but it did prevent a significant amount of IpaC aggregation. As in the absence of Tween-20, all of the IpaC Trp mutants appeared to have the same secondary structure content as native IpaC (data not shown).

The CD thermal unfolding profile of native IpaC shows that it undergoes a major secondary structure change as a function of temperature (data not shown). The observed changes in wild-type and mutant IpaC secondary structures begin at relatively low temperatures (data not shown); however, the melting temperature (T_m) appears to be about 60 °C for native IpaC, which is greater than that of any of the mutants (Table 6). Thus, in all cases, it appears that the incorporation of Trp into IpaC renders the protein at least slightly less thermally stable. With respect to each other, almost all the Trp mutants have similar stabilities with the exception of A106W and L154W, which have lower T_m values based on CD analysis (Table 6). This trend is also reflected in the initiation points of the thermal unfolding transitions (Table 6).

Because the fluorescence emission and quenching data may indicate that IpaC insertion into liposomes induces subtle conformational changes in IpaC, CD spectroscopy was used to determine the affect of membrane insertion on the overall secondary structure of IpaC (Figure 5). Relative to IpaC in aqueous solution (no Tween present), membrane incorporated IpaC appeared to actually gain secondary structure following liposome insertion (Figure 5) as indicated by the decreased ratio of the minima at 203 and 222 nm. These data suggest that some of the fluorescence data described above could be a result of changes in IpaC conformation caused by membrane insertion. It should be noted, however, that alterations in the oligomerization state of IpaC that could occur upon membrane interaction could also be responsible for the observed changes in secondary structure.

Monitoring IpaC Thermal Transitions by Second Derivative UV Analysis. Because of the aggregative nature of IpaC, low protein concentrations were used to monitor the thermal unfolding by CD spectroscopy. Nevertheless, the gradual aggregation of IpaC with increasing temperature precluded obtaining definitive T_m values based on CD analysis. Therefore, the approximate initial point of each melting transition is reported in Table 6 along with the computed apparent T_m. Due to difficulties in determining a precise T_m for the IpaC mutants by CD analysis, Trp derivative absorbance spectroscopy was also used to monitor thermal transitions in IpaC's structure. This method is useful for potentially aggregative proteins because it is less sensitive to spectral components such as light scattering because the light scattering component changes only graduatelly with wavelength, thus not perturbing derivative quantities. These spectra display two tryptophan minima, one of which is shared with tyrosine. For this investigation, the single tryptophan specific minimum was used to monitor thermal stability.

The data show that the microenvironments of the Trp residues at IpaC positions 106, 136, and 154 are the least thermally stable among the mutants (Figure 6). This is largely in agreement with the CD data, with the exception of F136W (Figure 6). The rest of the Trp mutants except R362W show similar initiation temperatures. Interestingly, the second derivative peak of the Trp residue at position 362 disappears at relatively low temperatures, making further determinations involving this residue impossible (Figure 6). This may be because of changes in the extent of overlap of peaks which arise from the protein's Tyr residues and the single Trp. The observed low unfolding temperatures for Trp mutants at positions 106 and 154 are consistent with the CD thermal unfolding results.

DISCUSSION

The ability of *S. flexneri* to invade and replicate in human intestinal cells is essential for the onset of shigellosis (*1*). The identified effector protein for cellular invasion by *S. flexneri* is IpaC (*7*, *12*), which also contributes to *Shigella*'s ability to destabilize its phagosomal membrane following host cell entry (*13*, *14*). To better understand IpaC's interaction with phospholipid membranes, its interaction with liposomes having different compositions was examined. Furthermore, IpaC was redesigned to contain single Trp residues at specific sites so that fluorescence, CD, and UV adsorption spectroscopies could be used to monitor the local environments of the introduced intrinsic fluorophores as a function of the conditions to which IpaC is exposed. A similar approach has been employed for a variety of proteins such as tear lipocalin (*20*), yeast Hsp104 (*38*), and myosin (*39*), among others. Relatively small shifts in the spectral properties of Trp residues provide a sensitive probe of local environment and changes in these environments.

Table 6: Summary of Data Obtained from Thermal Unfolding Experiments

Trp position:	IpaC	40	106	136	154	326	336	341	362
CD[a]	40−42[b]	40−42	23−35	40−42	25−27	42−44	40−42	40−42	40−42
CD T_m[c]	61.6 ± 3.8	54.9 ± 1.3	37.67 ± 0.2	52.6 ± 2.0	39 ± 1.4	54.5 ± 0.0	54.74 ± 0.36	50 ± 0.8	54.8 ± 2.9

[a] Because of potential aggregation problems, the reported temperature range is for the temperature at which the beginning of a thermal transition is observed. Assays were performed in all these experiments ≥3 times with the approximate range for the beginning of the thermal transition given. [b] All temperatures are given in °C. [c] T_m is the midpoint of the thermal unfolding as determined by CD spectroscopy.

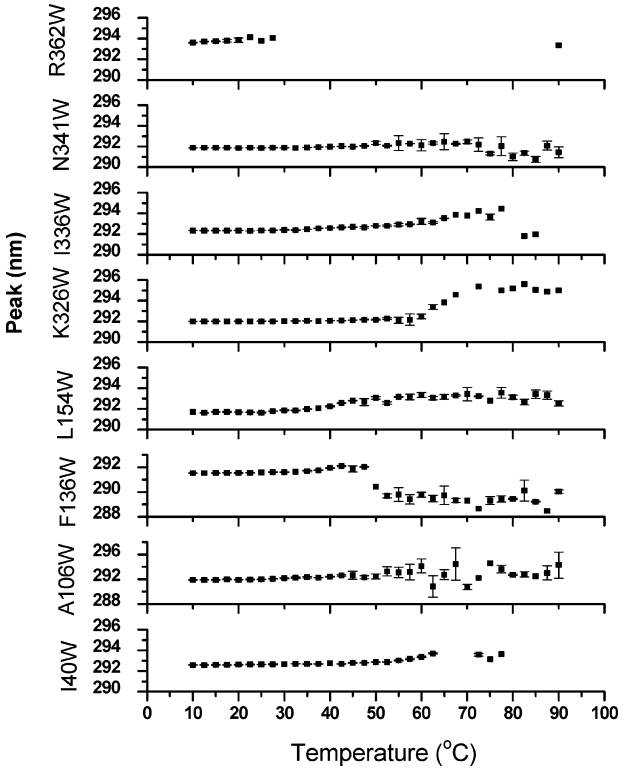

FIGURE 6: Effects of temperature on the position of the IpaC second derivative absorbance due to Trp. Data were collected at 2.5 °C intervals and processed as described in Experimental Procedures.

We have previously used deletion mutagenesis, complementation analyses, and in vitro binding studies to create a preliminary linear map that describes the functional organization of IpaC (Figure 1). IpaC's immediate N-terminus targets it for type III secretion while a separate region near the N-terminus is needed for association with the IpgC chaperone prior to export. Near the IpaC C-terminus is a predicted coiled-coil that is needed for *Shigella* contact-hemolysis activity and invasion functions. In contrast, the immediate C-terminus appears to be directly involved in IpaC's subversion of the signaling pathways that control the host cell cytoskeleton, but has no role in contact hemolysis (W. L. Picking and K. Flentie, unpublished data). Near the center of the IpaC sequence is a hydrophobic region that is required for IpaC interaction with phospholipid membranes (*15*) and in maintaining overall protein structure (*13*). Based on the functional map presented in Figure 1, specific sites were selected for Trp insertional mutagenesis as outlined in Experimental Procedures.

All but two of the IpaC single Trp mutants, N341W and R362W, permitted invasion of target cells at near wild-type levels. While these two mutants were essentially noninvasive, they were still capable of restoring substantial contact hemolysis to *S. flexneri* SF621. This suggests that there is a defect in effector function for these IpaC mutants, but not a defect in the ability to form pores, with IpaB, in the target cell membrane. This is a significant finding since these and other data suggest that the final 25 amino acids of IpaC are important for its invasion function, although the last 19 amino acids (outside the putative coiled-coil) appear to have no role in IpaC's contact-hemolysis activity. It is possible that the loss of invasion function for Trp mutants N341W and R362W is due to misalignment at the end of the putative coiled-coil region with accompanying structural disruption of the functionally important 19-amino acid tail. Alternatively, these IpaC mutants may experience difficulty in being recognized or exported properly by the *Shigella* TTSS. This would not appear to be the case since both mutant proteins accumulate at wild-type levels in culture supernatants (not shown) and known type III secretion signals are located N-terminally (*21*); however, such a possibility cannot yet be ruled out. In contrast, key residues within the coiled-coil region may contribute to both invasion and contact-hemolysis activities (*13*). In this study, S314W (upstream of the coiled-coil), K326W (within the coiled-coil), and N341W (at the end of the coiled-coil) all had reduced contact-hemolysis function (Table 1). These data support the proposal that IpaC's immediate C-terminus is critical for effector function, and the adjacent coiled-coil contributes to both invasion and contact-hemolysis functions.

All the IpaC Trp mutants caused the release of CF from liposomes containing a substantial acidic phospholipid component (data not shown), but the rate and extent of the IpaC−liposome interaction was greatly influenced by the presence of cholesterol. It has been shown that while IpaC interacts with membranes composed only of DOPC (*15*), it only causes disruption of membranes having an acidic phospholipid component (*13*, *18*). In contrast, the influence of cholesterol on IpaC association with membranes has not been tested despite the fact that the amount of cholesterol present in mammalian cell membranes can reach as high as 50% (*40*). The inclusion of 5% cholesterol in liposomes in this study was initially done to extend the lifetime of the liposomes; however, it was quickly recognized to have a negative impact on the rate with which IpaC caused CF release. This is of biological interest since many bacterial pore-forming toxins are attracted to membranes via their cholesterol component (*41*). Cholesterol has a role in maintaining membrane fluidity (*42*), reducing nonspecific permeability (*43*), and increasing the integrity of mammalian cell membranes (*44*). Interestingly, IpaC's overall ability to cause membrane disruption is enhanced by the presence of low concentrations of cholesterol. The amount of time taken to allow maximal fluorophore release, however, is increased by the presence of cholesterol. These data indicate that cholesterol content influences IpaC's ability to cause liposome disruption, but with consequences that vary depending upon the cholesterol level. It is possible that the increase in

membrane stability caused by cholesterol addition acts as a deterrent to IpaC-dependent membrane destabilization. To test this in the context of IpaC's interaction with eukaryotic cell membranes, it could be possible to isolate detergent-insoluble lipid rafts from cells before and after treatment with the cholesterol-depleting compound methyl-β-cyclodextrin.

In contrast to IpaC, IpaB's interaction with membranes does not appear to be negatively impacted by cholesterol content (data not shown) and it has been suggested that IpaB is a cholesterol-binding protein and that cholesterol is required for translocon function in target cells (*37*). The data suggest that the introduction of IpaB and IpaC at the host cell surface by *Shigella* involves a complicated array of protein−membrane interactions. Some of these may involve a rapid cholesterol-mediated interaction with IpaB combined with a slower but quantitatively significant interaction with IpaC. This is an intriguing possibility since *Shigella* invasion has been proposed to occur at lipid rafts (*35*, *36*), making the dynamics of IpaB and IpaC interactions with host cell membranes difficult to fully understand based solely on in vitro findings and using cells that have been compromised by chemical treatment. Nevertheless, IpaC's ability to interact with biological membranes is critical for *Shigella* entry into human cells and it is important for pathogen escape from its phagosomal vacuole.

All the Trp mutants were found to be useful as probes for determining the effect of membrane association on the local environment of different IpaC regions. The implications of these observations with respect to IpaC's incorporation into target cell membranes in vivo is not yet clear, and thus requires further study. Following incubation with liposomes, all of the incorporated Trp residues displayed blue shifts in their fluorescence emission maxima. The smallest shifts occurred for Trp at positions 40 and 154, while the largest occurred at the IpaC C-terminus. The apparent inability of the Trp at position 40 to enter the membrane was confirmed by fluorescence quenching analyses. Based on iodide quenching, the remaining Trp residues all demonstrated decreased exposure to the aqueous environment following liposome addition, although A106W and K326W were the most protected. This observation is consistent with the blue shifts seen for these IpaC mutants upon liposome addition, and it suggests that the first part of the IpaC hydrophobic region and a segment near the IpaC C-terminus demonstrate the most intimate interaction with liposomes. This certainly appears to be the case for the IpaC mutant A106W which is more efficiently quenched by 9,10 diBr-PC than by 6,7 diBr-PC, suggesting entry deep into the liposome bilayer interior. Regions near the IpaC C-terminus are either not quenched by these lipids or are quenched more readily by 6,7 diBr-PC, indicating either a less intimate interaction with the liposomes or one that is nearer the surface of the membrane.

It cannot be ruled out that some of the fluorescence properties seen here are a result of conformational changes that occur in IpaC following its association with liposomes composed of 50% DOPC and 50% DOPG. Indeed, when CD spectroscopy was used to examine the secondary structure content of IpaC in the absence and presence of liposomes, it appeared that the liposome-associated form of the protein had a larger amount of organized secondary structure than did the free protein. Based on the overall fluorescence data presented here (i.e. magnitude of blue shifts, partial protection from iodide, absence of quenching by diBr-PC lipids), it is possible that the increase in secondary structure can be attributed to the C-terminus of IpaC. This will require further investigation, but it appears that association with phospholipid membranes results in a stabilization of the putative coiled-coil near the IpaC C-terminus.

Analysis of thermally induced unfolding as monitored by CD shows that IpaC and its Trp mutants have similar or only slightly reduced stabilities except for the A106W and L154W mutants, which have significantly reduced T_m values (Table 6). Because there are potential problems with temperature-dependent aggregation of IpaC, it was difficult to quantitatively assess unfolding by CD spectroscopy. Therefore, second derivative UV absorbance experiments were used to confirm these data. Based on this method, which is less sensitive to protein aggregation, it appears that Trp incorporation into all three positions within the IpaC hydrophobic domain causes a minor decrease in protein stability. It should be noted, however, that CD spectroscopy provides a global picture of protein secondary structure while second derivative UV absorbance provides a more local picture of environmental changes occurring around, in this case, a single tryptophan residue.

Taken together, the data presented here suggest that the first part of the central hydrophobic region of IpaC is intimately involved in promoting interactions with phospholipid membranes, but that cholesterol influences this association. The IpaC C-terminus is also involved in membrane interactions, but may also undergo structural changes as a result of membrane association. This latter possibility may be related to the proposal that IpaC possesses a coiled-coil region near its C-terminus that may have a role in maintaining the C-terminal tail in a conformation that is compatible with triggering signals for uptake into target cells. Additional work with other mutant forms of IpaC will be needed to refine this initial low-resolution model of IpaC structure and function.

ACKNOWLEDGMENT

Technical assistance from Sarah Rome is gratefully acknowledged.

REFERENCES

1. Hale, T. L. (1991) Genetic basis of virulence in Shigella species, *Microbiol. Rev. 55*, 206−224.
2. Centers for Disease Control and Prevention (2005) *Shigellosis*, http://www.cdc.gov/ncidod/dbmd/diseaseinfo/shigellosis_g.htm.
3. Behrana, V., Harty, J. T., and Jones, B. D. (1998) Interactions of the invasive pathogens Salmonella typhimurium, Listeria monocytogenes, and Shigella flexneri with M cells and murine Peyer's patches, *Infect. Immun. 66*, 3758−3766.
4. Clerc, P., and Sansonetti, P. J. (1987) Entry of Shigella flexneri into HeLa cells: evidence for directed phagocytosis involving actin polymerization and myosin accumulation, *Infect. Immun. 55*, 2681−2688.
5. Niebuhr, K., and Sansonetti, P. J. (2000) Invasion of epithelial cells by bacterial pathogens the paradigm of Shigella, *Subcell. Biochem. 33*, 251−287.
6. Tran Van Nhieu, G., Bourdet-sicard, R., Dumenil, G., Blocker, A., and Sansonetti, P. J. (2000) Bacterial signals and cell responses during Shigella entry into epithelial cells, *Cell. Microbiol. 2*, 187−193.

7. Tran Van Nhieu, G., Caron, E., Hall, A., and Sansonetti, P. J. (1999) IpaC induces actin polymerization and filopodia formation during Shigella entry into epithelial cells, *EMBO J. 18*, 3249−3262.
8. Sansonetti, P. J., Ryter, A., Clerc, Pl., Maurelli, A. T., and Mounier, J. (1986) Multiplication of Shigella flexneri within HeLa cells: lysis of the phagocytic acuole and plasmid-mediated contact hemolysis, *Infect. Immun. 51*, 461−469.
9. Menard, R., Sansonetti, P. J., and Parsot, C. (1993) Nonpolar mutagenesis of the ipa genes defines IpaB, IpaC, and IpaD as effectors of Shigella flexneri entry into epithelial cells, *J. Bacteriol. 175*, 5899−5906.
10. Menard, R., Prevost, M. C., Gounon, P., Sansonetti, P., and Dehio, C. (1996) The secreted Ipa complex of Shigella flexneri promotes entry into mammalian cells, *Proc. Natl. Acad. Sci. U.S.A. 93*, 1254−1258.
11. Watarai, M., Funato, S., and Sasakawa, C. (1996) Interaction of Ipa proteins of *Shigella flexneri* with alpha5beta1 integrin promotes entry of the bacteria into mammalian cells, *J. Exp. Med. 183*, 991−999.
12. Marquart, M. E., Picking, W. L., and Picking, W. D. (1996) Soluble invasion plasmid antigen C (IpaC) from Shigella flexneri elicits epithelial cell responses related to pathogen invasion, *Infect. Immun. 64*, 4182−4187.
13. Kueltzo, L. A., Osiecki, J., Barker, J., Picking, W. L., Wessel, A., Picking, W. D., and Middaugh, C. R. (2003) Structure-function analysis of invasion plasmid antigen C (IpaC) from Shigella flexneri, *J. Biol. Chem. 278*, 2792−2798.
14. Osiecki, J., Barker, J., Picking, W. L., Barnoski-Serifs, A., Berring, E., Shah, S., Harrington, A., and Picking, W. D. (2001) IpaC from Shigella and SipC from Salmonella possess similar biochemical properties but are functionally distinct, *Mol. Microbiol. 42*, 469−481.
15. Tran, N., Serfis, A. B., Davis, R., Osiecki, J. C., Coye, L., Picking, W. L., and Picking, W. D. (2000) Interaction of Shigella flexneri IpaC with model membranes correlates with effects on cultured cells, *Infect. Immun. 68*, 3710−3715.
16. Kuwae, A., Yoshida, S., Tamano, K., Mimuro, H., Suzuki, T., and Sasakawa, C. (2001) Shigella invasion of macrophage requires the insertion of IpaC into the host plasma membrane. Functional analysis of IpaC, *J. Biol. Chem. 276*, 32230−32239.
17. Terajima, J., Moriishi, E., Kurata, T., and Watanabe, H. (1999) Preincubation of recombinant Ipa proteins of Shigella sonnei promotes entry of non-invasive Escherichia coli into HeLa cells, *Microb. Pathog. 26*, 223−230.
18. De Geyter, C., Vogt, B., Benjelloun-Touimi, Z., Sansonetti, P. J., Ruysschaert, J.-M., Parsot, C., and Cabiaux, V. (1997) Purification of IpaC, a protein involved in entry of Shigella flexneri into epithelial cells and characterization of its interaction with lipid membranes, *FEBS Lett. 400*, 149−154.
19. Picking, W. L., Coye, L., Osiecki, J. C., Serfis, A., and Picking, W. D. (2001) Identification of functional regions within invasion plasmid antigen C (IpaC) of Shigella flexneri, *Mol. Microbiol. 39*, 100−111.
20. Gasymov, O. K., Abduragimov, A. R., Yusifov, T. N., and Glasgow, B. J. (2001) Site-directed tryptophan fluorescence reveals the solution structure of tear lipocalin: evidence for features that confer promiscuity in ligand binding, *Biochemistry 40*, 14754−14762.
21. Harrington, A. T., Hearn, P. D., Picking, W. L., Barker, J. R., Wessel, A., and Picking, W. D. (2003) Structural characterization of the N terminus of IpaC from Shigella flexneri, *Infect. Immun. 71*, 1255−1264.
22. Provencher, S., and Glockner, J. (1981) Estimation of globular protein secondary structure from circular dichroism, *Biochemistry 20*, 33−37.
23. Sreerama, N., and Woody, R. W. (1993) A self-consistent method for the analysis of protein secondary structure from circular dichroism, *Anal. Biochem. 209*, 32−44.
24. Manavalan, P., and Johnson, W. C., Jr. (1987) Variable selection method improves the prediction of protein secondary structure from circular dichroism spectra, *Anal. Biochem. 167*, 76−85.
25. Pace, C. N. (1986) Determination and analysis of urea and guanidine hydrochloride denaturation curves, *Methods Enzymol. 131*, 266−280.
26. Raja, S. M., Rawat, S. S., Chattopadhyay, A., and Lala, A. K. (1999) Localization and environment of tryptophans in soluble and membrane-bound states of a pore-forming toxin from Staphylococcus aureus, *Biophys. J. 76*, 1469−1479.
27. Rausell, C., Munoz-Garay, C., Miranda-CassoLuengo, R., Gomez, I., Rudino-Pinera, E., Soberon, M., and Bravo, A. (2004) Tryptophan spectroscopy studies and black lipid bilayer analysis indicate that the oligomeric structure of Cry 1 Ab toxin from Bacillus thuringiensis is the membrane-inserted intermediate, *Biochemistry 43*, 166−174.
28. Stern, O., and Volmer, M. (1919) On the quenching time of fluorescence, *Z. Phys. 20*, 183−188.
29. Kueltzo, L. A., Ersoy, B., Ralston, J. P., and Middaugh, C. R. (2003) Derivative absorbance spectroscopy and protein phase diagrams as tools for comprehensive protein characterization: a bGCSF case study, *J. Pharm. Sci. 92*, 1805−1820.
30. Mach, H., and Middaugh, C. R. (1993) Measuring protein spectra in the presence of light scattering, *BioTechniques 15*, 240−242.
31. Richmond, J. Y., and McKinney, R. W., Eds. (1999) *Biosafety in Microbiological and Biomedical Laboratories*, 4th ed., U.S. Government Printing Office, Washington, DC.
32. Lakowicz, J. R. (1999) *Principles of Fluorescence Spectroscopy*, 2nd ed., Plenum Press, New York.
33. Pallen, M. J., Dougan, G., and Frankel, G. (1997) Coiled-coil domains in proteins secreted by type III secretion systems, *Mol. Microbiol. 25*, 423−425.
34. Eftink, M. R., Ionescu, R., Ramsay, G. D., Wong, C. Y., Wu, J. Q., and Maki, A. H. (1996) Thermodynamics of the unfolding and spectroscopic properties of the V66W mutant of Staphylococcal nuclease and its 1−136 fragment, *Biochemistry 35*, 8084−8094.
35. van der Goot, F. G., Tran Van Nhieu, G., Allaoui, A., Sansonetti, P., and Lafont, F. (2004) Rafts can trigger contact-mediated secretion of bacterial effectors via a lipid-based mechanism, *J. Biol. Chem. 279*, 47792−47798.
36. Lafont, F., Tran Van Nhieu, G., Hanada, K., Sansonetti, P., and van der Goot, F. G. (2002) Initial steps of Shigella infection depend on the cholesterol/sphingolipid raft-mediated CD44-IpaB interaction, *EMBO J. 21*, 4449−4457.
37. Hayward, R. D., Cain, R. J., McGhie, E. J., Phillips, N., Garner, M. J., and Koronakis, V. (2005) Cholesterol binding by the bacterial type III translocon is essential for virulence effector delivery into mammalian cells, *Mol. Microbiol. 56*, 590−603.
38. Hattendorf, D. A., and Lindquist, S. L. (2002) Analysis of the AAA sensor-2 motif in the C-terminal ATPase domain of Hsp104 with a site-specific fluorescent probe of nucleotide binding, *Proc. Natl. Acad. Sci. U.S.A. 99*, 2732−2727.
39. Yengo, C. M., Fagnant, P. M., Chrin, L., Rovner, A. S., and Berger, C. L. (1998) Smooth muscle myosin mutants containing a single tryptophan reveal molecular interactions at the actin-binding interface, *Proc. Natl. Acad. Sci. U.S.A. 95*, 12944−12949.
40. Sackmann, E. (1995) Biological membranes architecture and function, in *Structure and Dynamics of Membranes* (Lipowsky, R., and Sackmann, E., Eds.) pp 1−64, Elsevier, Amsterdam.
41. Gilbert, R. J. (2002) Pore-forming toxins, *Cell. Mol. Life Sci. 59*, 832−844.
42. Kusumi, A., Tsuda, M., Akino, T., Ohnishi, S., and Terayama, Y. (1983) Protein-phospholipid-cholesterol interaction in the photolysis of invertebrate rhodopsin, *Biochemistry 22*, 1165−1170.
43. Subczynski, W. K., Wisniewska, A., Yin, J.-J., Hyde, J. S., and Kusumi, A. (1994) Hydrophobic barriers of lipid bilayer membranes formed by reduction of water penetration by alkyl chain unsaturation and cholesterol, *Biochemistry 33*, 7670−7681.
44. Bloom, M., and Mouritsen, O. G. (1995) The evolution of membranes, in *Structure and Dynamics of Membranes* (Lipowsky, R., and Sackmann, E., Eds.) pp 65−95, Elsevier, Amsterdam.

BI0512593